

## THE REVERSE TURN AS A TEMPLATE FOR METAL COORDINATION

B. Imperiali,\* and T. M. Kapoor

Contribution no. 8753 from the Division of Chemistry and Chemical Engineering  
California Institute of Technology, Pasadena, California 91125, USA.

(Received in USA 3 March 1993)

*Abstract - The structural consequence of zinc binding to three octapeptides is examined. The experimental results indicate that placement of a constrained reverse turn motif in the core of the peptide nucleates the peptide secondary structure to facilitate metal coordination to ligands within the remainder of the sequence. These studies demonstrate that secondary structure in a polypeptide framework may be enhanced by a combination of  $\beta$ -turn nucleation and metal coordination.*

### Introduction

Preorganization is an important characteristic of metal binding sites in metalloproteins. This attribute is responsible for many important functions. For example, the blue copper proteins stabilize uncommon metal ion redox states, and in metal dependent hydrolases, expansion and contraction of the metal ion coordination sphere allow for participation in catalytic processes.<sup>1</sup> The structural and functional consequences of metal ion interaction with strongly coordinating side chains in peptide secondary structural motifs are less developed. The importance of metal coordination for structure enhancement has been demonstrated in the design of stable  $\alpha$ -helix motifs. Examples of exchange labile<sup>2</sup> and inert<sup>3</sup> systems, as well as use of natural and unnatural<sup>4</sup> metal ligands in the formation of organized, metal ion associated  $\alpha$ -helix structures, are documented. In contrast, there are to date no examples of metal coordination to induce  $\beta$ -sheet structure. This is surprising since metal ion coordination to residues in  $\beta$ -sheet structures in intact proteins is common. For example the metal coordination sites in the catalytic metalloproteins carbonic anhydrase and carboxypeptidase are localized exclusively on  $\beta$ -sheet or turn structures. Furthermore, catalytic function in these metalloproteins may be due in part to the order provided to the ligands by the peptide backbone.<sup>5</sup>

In the context of our long term goals in the *de novo* design and synthesis of functional metalloproteins we have chosen to investigate the influence of structural preorganization on

metal coordination in  $\beta$ -sheet and  $\beta$ -turn motifs. While the synthetic models by Kaiser<sup>6</sup> have clearly demonstrated the power of simple amphiphilic sequences to form  $\alpha$ -helices, little success has been achieved by corresponding models for  $\beta$ -sheets. The major problem in the *de novo* design of sheet motifs is that the favorable interactions that would pay the entropic price for folding are between residues that are *far apart* at the level of primary sequence.

### The $\beta$ -Turn as a Structural Nucleation Unit

$\beta$ -Turns are common in proteins, comprising on average 25% of the residues.<sup>7</sup> Since their recognition by Venkatachalam in 1968,<sup>8</sup> at least nine classes have been defined. The  $\phi$  and  $\psi$  angles of the (n+1) and (n+2) residues of the motif define the turn type.<sup>7</sup> The associated angles for the type II reverse turns are distinct from those of other structural motifs. Conformational selectivity can be achieved with this unit of secondary structure through use of a heterochiral peptide sequence.<sup>9</sup> We have recently demonstrated the tetrapeptide Ac-Val-Pro-D-Ser-His-NH<sub>2</sub> shows a significant amount of type II  $\beta$ -turn conformation in aqueous solution.<sup>10</sup> Our goal in the studies described herein is to examine the effect of incorporating this  $\beta$ -turn-forming sequence into peptides, in order to analyze its influence as a nucleating element for ordering metal ligands for coordination to divalent zinc. Table I shows the peptides examined in this study.

Table I Synthetic Peptides

| PEPTIDE | SEQUENCE   |
|---------|--|
| 1       | Ac-Glu <sup>1</sup> -Gly <sup>2</sup> - <u>Val</u> <sup>3</sup> - <u>Pro</u> <sup>4</sup> - <u>D</u> Ser <sup>5</sup> -His <sup>6</sup> -Thr <sup>7</sup> -His <sup>8</sup> -NH <sub>2</sub>         |
| 2       | Ac-His <sup>1</sup> -Gly <sup>2</sup> - <u>Val</u> <sup>3</sup> - <u>Pro</u> <sup>4</sup> - <u>D</u> Ser <sup>5</sup> - <u>His</u> <sup>6</sup> -Thr <sup>7</sup> -His <sup>8</sup> -NH <sub>2</sub> |
| 3       | Ac-His <sup>1</sup> -Gly <sup>2</sup> -Val <sup>3</sup> -Gly <sup>4</sup> -Gly <sup>5</sup> -His <sup>6</sup> -Thr <sup>7</sup> -His <sup>8</sup> -NH <sub>2</sub>                                   |

**Bold face amino acids**=> metal ligands; Underlined=> nucleating turn

The only strong metal ligands in the peptides examined are the imidazole and carboxylate groups. Water is expected to provide the remaining coordination to the metal center. Peptides 1 and 2 contain the structural nucleation unit Val-Pro-D-Ser-His and a potential metal binding site provided by residues (1), (6) and (8). Glycine was chosen to precede valine, allowing the third ligand to form a compact binding site without the steric hindrance produced by a substituted amino acid. Inclusion of the  $\beta$ -branched residue threonine (7) was designed to favor sheet character.<sup>11</sup> Peptide 3, lacking the prolyl-D-seryl core, was designed to test the impact of the nucleating turn on metal coordination. The conformational flux of this control peptide, compared to that observed for turn-containing peptides, provides a measure of the nucleating power of the turn.

In these studies, the role of the metal binding site is to serve as a device that will *further* facilitate the ordering of the peptide conformation. We demonstrate that when appropriate residues are localized within the remainder of the sequence that the structure nucleated by the type II turn serves as a template for metal coordination. In this case we provide evidence for the formation of a  $\beta$ -hairpin structure. Without the nucleating structure, high affinity metal coordination is absent and enhanced order is not achieved.

### Experimental Section

**Peptide Synthesis and Characterization.** Commercially available starting materials and reagents for peptide synthesis were purchased from MilligenBiosearch or Sigma Chemical Co. Peptides were synthesized on a 0.1-0.2 mmole scale by solid phase methods using N $^{\alpha}$ -9-fluorenylmethyloxycarbonyl (Fmoc) protected amino acids<sup>12</sup> and benzotriazol-1-yloxytris(dimethylamino)phosphoniumhexafluorophosphate/1-hydroxybenzotriazole (BOP/HOBT)<sup>13</sup> mediated amide coupling chemistry on a Milligen 9050 automated peptide synthesizer. PAL resin<sup>14</sup> (Milligen GEN077483 substituted at ca. 0.30 meq/g) was used to afford carboxyl terminus primary amides. Activated esters were formed *in situ* using BOP, HOBT and 0.451 M N-methylmorpholine in dimethylformamide (DMF). A typical protocol involved a 2h coupling time with four equivalents of amino acid. Deprotection of Fmoc-protected amine groups was performed using a 7 min. 20% piperidine/DMF wash. Peptides were N-acetylated on the resin using 20 equivalents of acetic anhydride and 5 equivalents of triethylamine in 3 mL DMF. After shaking for 2 h, the resin was washed with dichloromethane and vacuum dried.

Peptides were deprotected and cleaved from the resin by treatment with trifluoroacetic acid (TFA)/thioanisole/ethanedithiol/anisole (90:5:3:2) for two hours. After filtration of the resin, the combined filtrates were concentrated to ca. 2 mL volume and precipitated with ether/hexane 2:1. The supernatant was decanted and the peptides triturated with ether/hexane 2:1 (3 x 20 mL). The peptides were repeatedly lyophilized until no traces of the cleavage mixture remained. Peptides were purified, when necessary, using reverse phase HPLC (C<sub>18</sub>) Gradient elution with 0.08% TFA in acetonitrile added to 0.1% TFA in water.

Typical characterization of each peptide includes <sup>1</sup>H NMR in both DMSO-*d*<sub>6</sub> and 10% D<sub>2</sub>O/90% H<sub>2</sub>O, RPHPLC analysis and high resolution mass spectroscopy.

**NMR Studies.** NMR experiments were run on a Bruker Instruments AMX500 spectrometer. Spectra in H<sub>2</sub>O/D<sub>2</sub>O mixtures are internally referenced to dimethylsulfoxide (DMSO) at 2.72 ppm. The shift of DMSO in aqueous solvents has been calibrated using 3-(trimethylsilyl)propionic-2,2,3,3-*d*<sub>4</sub> acid sodium salt. Peak assignments were made with a two-dimensional total correlation spectroscopy TOCSY experiment. The TOCSY FID's were multiplied by a phase shifted sine bell apodization function prior to Fourier transformation.

Nuclear Overhauser effects (NOE's) were detected using the 2D spin-locked ROESY experiment.<sup>15</sup> It should be noted that the ROESY cross peaks, while useful in obtaining qualitative proximity information (<3.5 Å) cannot be easily used to derive quantitative distance information in the same way as 2D NOE spectroscopy (NOESY) data.<sup>16</sup> 2D ROESY experiments were run in phase sensitive mode using time proportional phase increments. For the ROESY experiments the spin lock power setting was calculated by determining the power of a 125  $\mu$ s 90° pulse. The experimental parameters were varied to optimize amide cross peak intensity and to minimize HOHAHA artifacts.<sup>17</sup> The FID's were multiplied by a phase shifted squared sine bell apodization function prior to Fourier transformation. In a typical ROESY experiment the relaxation delay was 1.3 s and the transmitter offset was positioned in the center of the spectrum or on the water resonance and the data matrix consisted of 512  $t_1$  increments containing 2K complex points. For all experiments run in 90% H<sub>2</sub>O/10% D<sub>2</sub>O, solvent suppression was obtained using presaturation at 280K.

The temperature dependence of the amide proton shifts was determined between 280 K and 310 K. A minimum of five temperature steps were recorded in each experiment. Calibration of the probe temperature was performed using either a methanol or ethylene glycol standard. In all cases, the chemical shifts were found to vary linearly with temperature.

Zinc titrations were carried out at pH 7.5 in Tris-d<sub>11</sub> buffer (concentration 100 mM) in D<sub>2</sub>O by additions of 100 mM ZnCl<sub>2</sub> solution also in D<sub>2</sub>O. The peptide concentrations were 7.5 mM and the experiments were carried out at 323 K.

**CD Studies.** CD spectra were recorded on a Jasco J-600 Spectropolarimeter equipped with a temperature regulation device. Peptide solutions were prepared in double-distilled H<sub>2</sub>O (typical concentration range: 25-50  $\mu$ M) and degassed using 4 freeze-pump-thaw cycles and stored under dry nitrogen. Standard peptide spectral samples were prepared by serial dilution with double-distilled H<sub>2</sub>O (degassed by nitrogen sparging for 1 h) and analyzed in a 1.0 cm path length quartz cell. Zinc titrations were carried out at pH 7.5 in Tris buffer (500  $\mu$ M) solution using a 5 mM stock of ZnCl<sub>2</sub> solution in double-distilled H<sub>2</sub>O. pH dependent titrations were carried out in the absence of buffer. The presence of 50 mM NaCl did not effect the titrations. All spectra were obtained from 350 nm to 200 nm at a scan speed of 50 nm/min, a time constant of 0.5 s, and a bandwidth of 1 nm. In all cases a minimum of 8 scans was taken. CD spectra are reported in ellipticity/ $\alpha$ -amino acid residue. Data were processed on a Macintosh IICI computer with KaleidaGraph software, version 2.1.1. CD studies were also carried out under the conditions (concentration and temperature) of the NMR experiments to ensure the absence of aggregative effects.

## Results and Discussion

Three independent experimental criteria are used to establish the conformational predilections of the peptides in aqueous solution. These include an evaluation of nuclear Overhauser effects, amide temperature coefficients and circular dichroism spectra. In the ROESY experiment, peptides 1 and 2 showed the  $d_{NN}$  (Ser<sup>5</sup>, His<sup>6</sup>),  $d_{\alpha N}$  (Ser<sup>5</sup>, His<sup>6</sup>),  $d_{\alpha\delta}$  (Val<sup>3</sup>, Pro<sup>4</sup>) and the  $d_{\alpha N}$  (Pro<sup>4</sup>, Ser<sup>5</sup>) connectivities. The presence of the connectivity between the amide protons of the (n+2) and the (n+3) residues is diagnostic of the turn since it can only be observed if there is a sufficient population of the peptide in the "folded" conformation. The  $d_{\alpha\delta}$  (Val<sup>3</sup>, Pro<sup>4</sup>) connectivity provides evidence that the Pro<sup>4</sup> is in the trans conformation. In addition,  $d_{\alpha N}$  (Pro<sup>4</sup>, Ser<sup>5</sup>) connectivity specifically supports a type II turn.<sup>18</sup> For peptide 2, a strong connectivity  $d_{NG}$  (His<sup>1</sup>, Val<sup>3</sup>) is also seen. This may imply that the peptide in solution has its N-terminus 'kinked' and folded back. The NMR data further shows that the peptide does not have any significant sheet conformation in the absence of metal ions, since diagnostic long range connectivities between the two anti parallel strands are not seen. The ROESY spectrum of peptide 3 does not reveal any structurally diagnostic NOE effects.

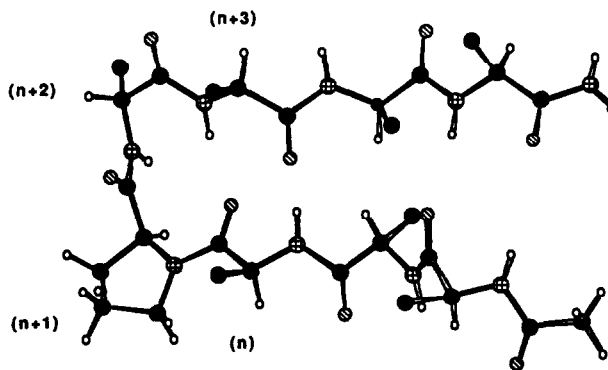


Figure 1. Schematic of Octapeptide in Type II  $\beta$ -turn (Key:  $\circ$ :H;  $\bullet$ :C;  $\ominus$ :O;  $\oplus$ :N;  $\bullet$ :R)

The temperature coefficients for the amide proton resonances provide an indication of which amides are experiencing a solvent shielded (hydrogen-bonded) environment. Temperature coefficients are influenced strongly by solvent effects; in water, the absolute values range from (-)2 -> (-)11 ppb/K [(-)4 ppb/K suggests strong solvent shielding, (-)4 -> (-)6 ppb/K moderate shielding and >(-)6 ppb/K indicates that a proton is likely to be exposed to the bulk solvent]. Peptide 3 appears devoid of any secondary structural elements; all temperature coefficients are >(-)7 ppb/K. In contrast, in peptides 1 and 2 the histidine (6) amide proton is clearly solvent shielded with temperature coefficients <(-)4 ppb/K. In a  $\beta$ -turn,

the (n+3) amide NH, in this case histidine (6), would be involved in a hydrogen bonding interaction with the carbonyl group of the (n) residue, and therefore, would be expected to experience a solvent shielded environment.

**Table II**

**Temperature Coefficients for Amide Proton Resonances in Water (no metal)**

| PEPTIDE | $(\Delta\delta/\Delta T)/\text{ppb/K}$ |           |          |
|---------|--|-----------|----------|
|         | (n)                                    | (n+2)     | (n+3)    |
| 1       | -6.8 (V)                               | -8.4 (DS) | -3.3 (H) |
| 2       | -7.7 (V)                               | -9.2 (DS) | -3.8 (H) |
| 3       | -7.1 (V)                               | -7.1 (G)  | -7.2 (H) |

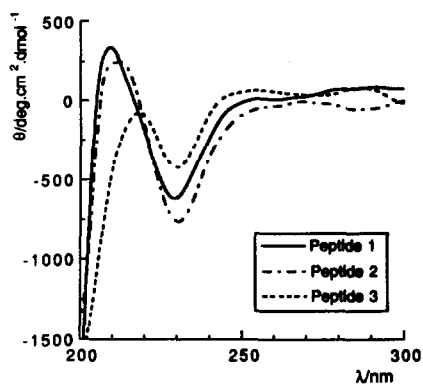


**Figure 2** CD Spectra of peptides 1, 2 and 3; 50 $\mu\text{M}$ , 25 $^{\circ}\text{C}$  pH 7.5.

Further information regarding the solution state conformation of the peptides is derived from CD studies.<sup>19</sup> In the absence of metal, the CD spectrum for peptides 1 and 2 is characterized by negative ellipticities  $>220\text{nm}$  and  $<190\text{nm}$  and a positive ellipticity in the 200-210nm range (as shown in Figure 2). These minima and maxima are consistent with the assignment of a type II  $\beta$ -turn structure in solution. The almost superimposable curves for the two peptides imply that they have essentially identical conformational profiles in solution. In contrast, the CD spectrum of peptide 3, indicates a lack of secondary structure.

Since spectra of specific peptide secondary structure motifs are quite distinct,<sup>19</sup> circular dichroism can be employed as an assay for the effect of metal coordination on peptide conformation in solution. As illustrated in Figure 3a, the ellipticity maximum for the peptide 2 both shifts to shorter wavelengths and greatly increases in intensity on addition of divalent zinc. This effect is subject to saturation; indicating that the metal binding site becomes filled at levels consistent with the affinity of the peptide for the divalent cation. At appropriate concentrations ( $>50\mu\text{M}$ ) saturation is achieved at a 1:1 metal:peptide stoichiometry. CD spectral data for peptide 2, collected at varying concentrations (50 $\mu\text{M}$ -5mM), are virtually identical; similar effects are observed with peptide 1. This provides evidence that aggregation effects are not

significant. Although precise calculations of the binding constants of the metal-peptide complexes require further experiments, preliminary analysis (from the titration curve in Figure 3b) shows that the dissociation constants for peptides 1 and 2 with zinc are 20 and 12.5  $\mu\text{M}$  respectively. This slight variation in binding likely reflects the different coordinating properties of carboxylate and imidazole ligands<sup>20</sup> in addition to geometrical constraints imposed by the peptide backbone. While the ideal CD spectra for pure  $\beta$ -sheet structures generally show an absorption maximum at a shorter wavelength, it is important to remember that some contribution of the CD spectrum comes from the  $\beta$ -turn motif within the supersecondary structural element. While the data illustrated does not provide conclusive proof of the transition of the peptide conformations from a turn to a sheet, it does imply is that there is a significant *ordering* of the peptide conformation upon metal binding. Analogous results are obtained on titration of  $\text{Co}^{\text{II}}$  with peptides 1 and 2.

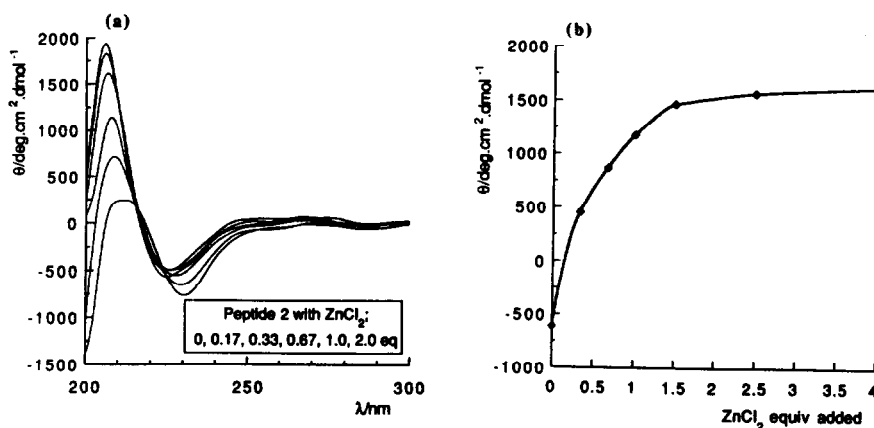


**Figure 3.** Interaction of peptide 2 with  $\text{ZnCl}_2$

- (a) 50  $\mu\text{M}$  peptide 2, 25 $^\circ\text{C}$  pH 7.5; 200-300 nm scan addition of  $\text{ZnCl}_2$  as indicated in legend.  
 (b) 25  $\mu\text{M}$  peptide 2, 25 $^\circ\text{C}$  pH 7.5; ellipticity changes at 206 nm on addition of  $\text{ZnCl}_2$ .

The zinc titration for peptide 3 is shown in figure 4. This peptide does not appear to undergo any significant conformational change on addition of metal. This study has been repeated over a wide range of concentrations and it is clear that, under similar conditions, peptide 3 is unable to undergo the dramatic changes conformational changes seen with peptides 1 and 2. Whether the above difference in metal interaction is primarily a structural effect and not a result of a change in the primary peptide sequence is tested in the following way. A pH dependent zinc titration of the peptides showed that metal binding was greatest near pH 7, but not observed at all below pH 5.5. These results indicate that the metal interaction is dependent

on the protonation of the imidazole ring nitrogens; thus at low pH, protons compete with metal for imidazole coordination. The interaction of  $ZnCl_2$  with peptides 1 and 2 was unaffected by varying ionic strength (0-0.1M) and in the presence and absence of Tris buffer salts.

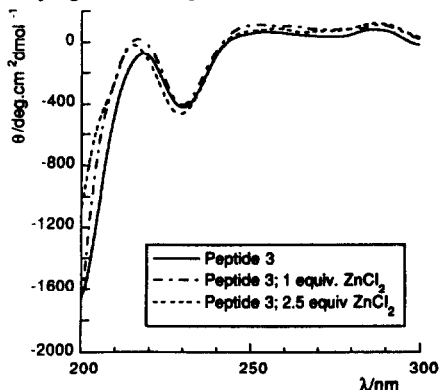


**Figure 4** Interaction of peptide 3 (50  $\mu$ M, 25°C pH 7.5) with  $ZnCl_2$

Additional evidence illustrating that the interaction is primarily between the imidazole rings and the metal ions can be obtained from NMR. TOCSY experiments at pH 7 show that the six imidazole ring protons and the six histidine  $\beta$ - $CH_2$  protons, shift significantly upon the addition of metal. No other metal dependent shifts are observed, indicating that coordination to the backbone amides is not occurring at these concentrations.

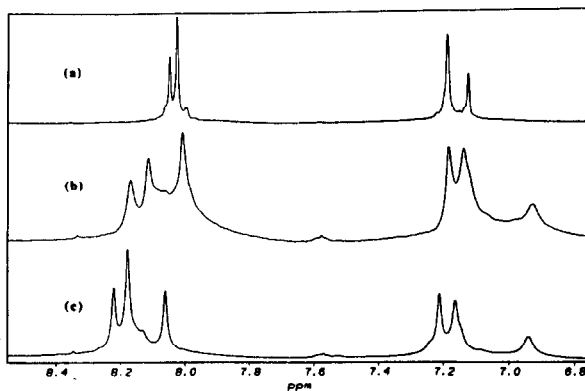


**Figure 5**  $^1H$  NMR of imidazole ring protons on addition of  $ZnCl_2$  to peptide 2 (7.5 mM, 25°C pH 7.5) (a) 0 mM  $ZnCl_2$ ; (b) 3.75 mM  $ZnCl_2$ ; (c) 11.25 mM  $ZnCl_2$ .

Unfortunately, the pH dependency on the metal binding limits the usefulness of any NOE experiments, since at the pH where metal binding is effective, proton exchange is too rapid to allow observation of diagnostic NOE's between amide NH protons and other constituents of the polypeptide. To further probe the interaction between the imidazole donors



and the metal ion, the effect of zinc dichloride titration on the peptide in D<sub>2</sub>O was examined. The spectra show that the imidazole groups on peptide 2 do indeed interact with the metal as evidenced by shifting of the imidazole resonances on the addition of a single equivalent of zinc (illustrated in Figure 5). Parallel experiments with peptide 3 reveal that addition of *several* equivalents of zinc is required to bring about changes in the proton NMR spectrum. These observations together with the CD results for peptide 3 suggest that at the elevated concentrations employed for the NMR experiment metal ion/imidazole association does occur, however, it does not afford a discrete peptide/metal ion complex.

## Conclusions

Spectroscopic studies on the binding of zinc to peptides 1 and 2 reveals that, at low concentrations, metal ion induces the formation of a new ordered structure. CD studies strongly suggest the presence of a  $\beta$ -hairpin structure. NMR indicates binding of all three histidine imidazole rings in the coordinated complex at neutral pH. In contrast, peptide 3 shows quite distinct behavior, and fails to adopt any additional order on metal binding. The results imply that metal coordination alone does not provide a sufficient driving force to enable the peptide to overcome 'activation barrier' for the folding process. While, in general, the rules for determining what constitutes a sufficient nucleating center for the induction of enhanced metal binding properties are not complete, the potential of the constrained type II turn in this case is clear.

## Acknowledgments

This work was supported by the National Science Foundation (CHE 9104445) and the Summer Undergraduate Research Fellowship (SURF) Program at Caltech. Generous support from Monsanto Chemical Company is also gratefully acknowledged.

## References

1. Vallee, B. L.; Williams, R. J. P. *Proc. Natl. Acad. Sci. U.S.A.* **1968**, *59*, 498.
2. Ghadiri, M. R.; Choi, C. *J. Am. Chem. Soc.* **1990**, *112*, 1630.
3. Ghadiri, M. R.; Fernholz, A. K. *J. Am. Chem. Soc.* **1990**, *112*, 9633.
4. Ruan, F.; Chen, Y.; Hopkins, P. B. *J. Am. Chem. Soc.* **1990**, *112*, 9403.
5. Williams, R. J. P. *Polyhedron*, **1987**, *6*, 61.
6. Kaiser, E. T.; Kedzy, F. J. *Proc. Natl. Acad. Sci. U.S.A.* **1983**, *80*, 1137.
7. For a recent review see: Rose, G. D.; Gierasch, L. M.; Smith, J. A. *Adv. Protein Chem.* **1985**, *37*, 1.
8. Venkatachalam, C. M. *Biopolymers*, **1968**, *6*, 1425.

9. Aubry, A.; Cung, M.T.; Marraud, M. *J. Am. Chem. Soc.* **1985**, *107*, 7640.
10. Imperiali, B.; Fisher, S. L.; Moats, R. A.; Prins, T. J. *J. Am. Chem. Soc.* **1992**, *114*, 3182.
- 11a. Levitt, M. *Biochemistry*, **1978**, *17*, 4277. b. Chou, P. Y.; Fasman, G. D. *Biochemistry*, **1974**, *13*, 211.
- 12a. Atherton, E.; Fox, H.; Harkiss, D.; Sheppard, R. C. *J. Chem. Soc., Chem. Commun.* **1978**, 539. b. Carpino, L. A.; Han, G. Y. *J. Org. Chem.* **1972**, *37*, 3404.
13. Hudson, D. *J. Org. Chem.* **1988**, *53*, 617.
14. Biosearch Technical Bulletin No. 9000-02.
- 15a. Bothner-By, A. A.; Stephens, R. L.; Lee, J., Warren, C. D.; Jeanloz, R. W. *J. Am. Chem. Soc.* **1984**, *106*, 811. b. Bax, A. *J. Magn. Reson.* **1988**, *77*, 134. c. Bax, A.; Davis, D. G. *J. Magn. Reson.* **1985**, *63*, 207.
16. Bauer, C. J.; Frenkiel, T. A.; Lane, A. N. *J. Magn. Reson.* **1990**, *87*, 144.
17. Cavanagh, J.; Keeler, J. *J. Magn. Reson.* **1988**, *80*, 186.
18. Wuthrich, K.; Billeter, M.; Braun, W. *J. Mol. Biol.* **1984**, *180*, 715.
- 19a. Woody, R. W. *Peptides, Polypeptides and Proteins*, Blout, E. R.; Bovey, F. A.; Goodman, M.; Lotan, L. Eds.; Wiley, New York, N. Y., 1974, p.338. b. Manning, M. C.; Illangasekare, M.; Woody, R. W. *Biophys. Chem.* **1988**, *31*, 77.
20. Martin, R. B. *Metal Ions in Biological Systems, Volume 9: Amino Acids as Ambivalent Ligands*, Sigel, H. Ed.; Marcel Dekker, Inc., New York and Basel, 1979, p.6.